Clays and Clay Minerals, Vol. 58, No. 6, 792–802, 2010.

CHARACTERIZATION OF ORGANO-BENTONITES OBTAINED FROM DIFFERENT LINEAR-CHAIN QUATERNARY ALKYLAMMMONIUM SALTS

İLKER ERKAN[1], İBRAHIM ALP[1,*], AND MEHMET SABRİ ÇELİK[2]

[1] Karadeniz Technical University, Department of Mining Engineering, Trabzon, Turkey
[2] İstanbul Technical University, Department of Mineral Processing Engineering, İstanbul, Turkey

Abstract—The effects of surfactants on bentonites have been of great scientific interest for many years. Even though quaternary alkylammonium salts (QAS) have been studied, very few data are available on the comparative performance of different chain-length QAS for the modification of the surface properties and adsorption properties of bentonites. The objective of this study was to investigate the effect of chain length on the adsorption of cationic surfactants onto bentonite. The surface and adsorption properties of different chain-length QAS, *i.e*. hexadecyltrimethylammonium bromide (HTAB, C16), tetradecyltrimethylammonium bromide (TTAB, C14), and dodecyltrimethylammonium bromide (DTAB, C12), to produce organo-bentonites (OB) were studied. The concentrations of QAS were selected based on the cation exchange capacity (CEC) of the clay mineral. Zeta potential, swelling, and viscosity measurements and scanning electron microscopy (SEM), X-ray diffraction (XRD), and Fourier-transform infrared (FTIR) analyses were used to explain the changes in surface properties. The results indicated that the best modification of bentonite was obtained using a 16-carbon chain length QAS (HTAB) in a 1:1 ratio of QAS to CEC. The basal spacing at this concentration was measured to be 22.19 Å, which also corresponded to the maximum adsorption density. The OB produced at this concentration showed the best hydrophobic character based on the swelling tests in toluene. The extent of hydrophobicity and adsorption density was correlated with the CEC and alkyl chain of the QAS. All these properties were used to elucidate the mechanism of modification governing the bentonite/QAS system.

Key Words—Adsorption, Cation Exchange Capacity (CEC), Chain-length, Electrokinetics, Organo Bentonite, Rheology.

INTRODUCTION

Organo-clays (OC) have recently become very important materials in commercial uses due to their large surface area, specific active sites, suspension abilities, and attractive adsorption properties. Organo-clays are used in many industrial applications such as thickening agents in inks and paints, as thickening/suspending/thixotropic additives in cosmetic formulations (Patel *et al.*, 2006), adhesives, drilling fluids (Kirsner *et al.*, 2003), as gelling agents in lubricants (Faci, 2001), and as ingredients to form nanocomposites (Lan and Pinnavaia, 1994). Organo-clays are commonly prepared using natural smectites such as montmorillonite or hectorite (Vougaris and Petridis, 2002; Can *et al.*, 2007; Erkan *et al.*, 2008; Paiva *et al.*, 2008). In addition to smectites, synthetic fluoro-hectorite (Gorassi *et al.*, 2003), sepiolite (Sabah *et al.*, 1998), clinoptilolite (Ersoy and Çelik, 2003), and synthetic micas (Klapyta *et al.*, 2003) are also used. Electrokinetics, rheological properties, and surface properties of montmorillonite can be modified conveniently using alkyl ammonium salts, which convert the surface of the clay from hydrophilic to hydrophobic through the exchange of interlayer cations with alkylammonium cations. This modified material is a clay-surfactant hybrid material (Favre and Lagaly, 1991; Akın and Çelik, 1995; Paiva *et al.*, 2008) and is typically referred to as organo-montmorillonite or organo-bentonite (OB).

In industrial production, bentonite is treated with QAS either with small amounts of water (paste-like materials) or in more diluted dispersions. The amount of QAS added corresponds to the experimental cation exchange capacity (CEC) or to the predetermined multiples of the CEC (Lagaly *et al.*, 2006; Erkan, 2008). The chain length of QAS dictates whether the surface can acquire sufficient hydrophobicity (Lagaly, 1986; Klapyta *et al.*, 2001; Frost *et al.*, 2007; Paiva *et al.*, 2008). Generally, OC studies in the literature reveal that QAS increases the hydrophobicity of the clay (Baldassari *et al.*, 2006; Marras *et al.*, 2007). The replacement of inorganic cations with QAS cations having a long carbon chain (generally C10 to C22) reduces the hydration of the clay (Baldassari *et al.*, 2006) and the resulting material can swell and disperse in organic fluids. Generally, QAS having <12 carbons in the chain are not used to produce an OC because they fail to impart the desired level of hydrophobicity. Therefore, alkyl chain lengths of 16 and 18 are usually preferred (Yang *et al.*, 2002; Ersoy and Çelik, 2003).

* E-mail address of corresponding author:
ialp@ktu.edu.tr
DOI: 10.1346/CCMN.2010.0580607

Many researchers have studied OC produced from different QAS (Lee *et al.*, 1989; Smith *et al.*, 1990; Medrzycka and Zwierzykowski, 2000; Xi *et al.*, 2005; Forland and Blokhus, 2007; Paiva *et al.*, 2008) and other surfactants (Xie *et al.*, 2001; Vazquez *et al.*, 2008). Modification of montmorillonites with QAS and the characterization of surface and adsorption properties of the resultant OB have received the most attention in recent years (Zhu *et al.*, 2007; Vazquez *et al.*, 2008; Nuntiya *et al.*, 2008; Sompech *et al.*, 2008). Specifically, modified montmorillonites were produced for use in areas such as adsorbents for removing organics from waters, nanofillers for nanocomposite production, and thickening agents for paints (Zhu *et al.*, 1997; Liu *et al.*, 2005). The most preferred alkylammonium cations in these studies are dodecyltrimethylammonium bromide (DTAB, C12), tetradecyltrimethylammonium bromide (TTAB, C14), hexadecyltrimethylammonium bromide (HTAB, C16), and octadecyltrimethylammonium bromide (OTAB, C18) (Tjandra *et al.*, 2006; Mohammad and Bhawani, 2008). Even though these QAS cations have been studied, few data are available on the comparative performance of DTAB, TTAB, and HTAB for the modification of the surface and adsorption properties of montmorillonite.

The aim of this study was, therefore, to compare and characterize the DTAB, TTAB, and HTAB surfactant-modified OB where adsorption of these three QAS (with different chain lengths) on Na^+ bentonite was measured. The zeta potential, swelling, and viscosity of the OB produced were also determined to explain the change in electrokinetic, rheological, adsorption, and surface properties of the OB, depending on the QAS chain length. X-ray diffraction (XRD) and Fourier-transform infrared (FTIR) analyses were performed to further discuss the success and extent of exfoliation of OB.

MATERIALS AND METHODS

Materials

The Na^+-bentonite used in this study was supplied by Samaş Bentonite Corp. (Reşadiye, Tokat, Turkey). The raw bentonite with a 72 meq/100 g CEC was purified through a multi-stage washing and classification process using a hydrocyclone (Boylu *et al.*, 2007). The purified Na^+-bentonite sample with a CEC of 98 meq/100 g was dried at 60ºC in an oven and then re-ground and sieved to <150 μm using a laboratory-type sieve (Retsch) in preparation for subsequent use. The 50% passing (d_{50}) size of the purified bentonite was determined at 3 μm using a Fritsch particle-size analyzer (Figure 1). The chemical analysis of the purified bentonite was 68.14% SiO_2, 23.87% Al_2O_3, 0.24% CaO, 2.53% MgO, 0.16% K_2O, 2.45% Na_2O, and 2.61% Fe_2O_3. The elemental composition of purified bentonite was estimated as $[(Na_{0.56}K_{0.02}Ca_{0.03})[Si_{7.98}Al_{0.02}](Al_{3.27}Fe_{0.23}Mg_{0.44})O_{20}(OH)_4]$. The QAS used in the preparation of the OB were DTAB ($CH_3(CH_2)_{11}N(CH_3)_3Br$), TTAB ($CH_3(CH_2)_{13}N(Br)(CH_3)_3$), and HTAB ($CH_3(CH_2)_{15}N(Br)(CH_3)_3$). The former two were obtained from Sigma whereas the latter from Merck as ACS certified powder reagent. These QAS were used as received without any purification.

Methods

The QAS were dissolved in water to prepare a 0.2 mol/L stock solution for successive dilution as necessary. The purified Na^+-bentonite was dispersed in water at 3% (w/w) and agitated by a magnetic stirrer at 60ºC for 1 h. After dispersion, the suspension cooled to room temperature (25ºC ±3ºC). A predetermined amount of a selected QAS was then added and the mixture was stirred for 2 h. Thereafter, the mixture was filtered and

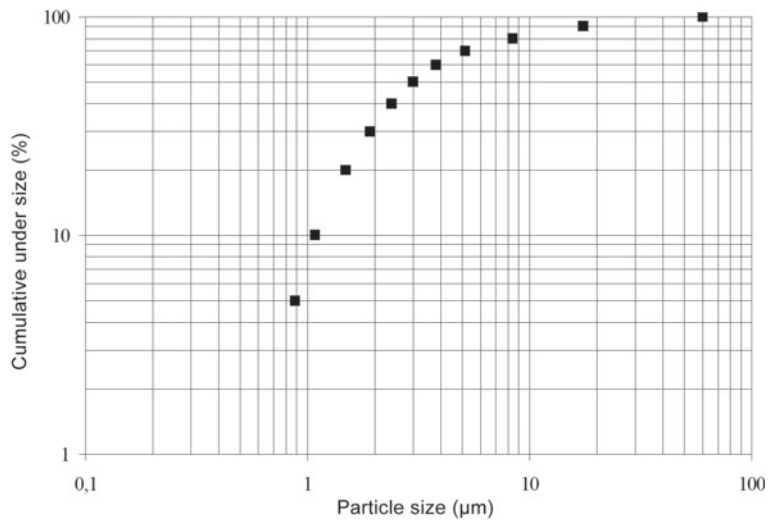

Figure 1. Particle-size distribution of purified Reşadiye bentonite.

rinsed with fresh distilled water to remove the desorbed QAS residue. The filter cake was then dried in an oven at 60ºC, ground with an agate mortar and pestle to <150 μm particle size before use. The suspensions prepared were also used to determine the amount of adsorption, electrokinetics, and rhelogical properties. This procedure was repeated for all QAS and concentrations.

The rheological properties of suspensions were determined using a Brookfield DV II Viscosimeter (Brookfield, Essex, UK). Following measurement of the viscosity, the OB suspension was centrifuged to obtain a clear supernatant liquid. The solid product and the supernatant were used to determine the electrokinetic properties (using a Zeta-Meter+3 (Sabah *et al.*, 2007)) and the adsorption properties of QAS (by the two-phase titration method), respectively. This method was based on the interaction of an anionic surfactant (SDS; sodium dodecyl sulfate) with the cationic alkylammonium in the presence of chloroform (Reid *et al.*, 1967). The method exploits the color change of the aqueous phase from blue to pink. The adsorption density was calculated from the consumption of anionic surfactant at the end point. A calibration curve for each concentration was constructed to calculate the unknown surfactant concentration.

The swelling behavior of OB was determined at different polarities. Water and toluene were used as the most and the least polar media, respectively. Acetone was added to toluene (50% v/v) to vary the polarity. The swelling tests were conducted with 3 g of OB in 10 mL graduated glass tubes. The OB were fed to the liquid slowly and left stationary for 24 h before taking the measurements.

The XRD patterns of the unmodified clays were recorded between 2º2θ and 40º2θ at a scanning speed of 2º2θ /min at a step size of 0.05º2θ, using a Rigaku D/max-IIIC X-ray diffractometer with CuKα (1.54 Å) radiation. In addition, the XRD analysis of the OB powder was performed under the same conditions except for the recording range (2−10º2θ). The XRD analysis was performed to show the structural differences between modified and unmodified bentonite and the corresponding change of the basal spacing. A JEOL JSM 6400 scanning electron microscope (SEM) was used to observe the differences in surface morphologies between modified and unmodified bentonite. Fourier-transform infrared analysis was carried out using a Perkin Elmer model Spectrum One spectrophotometer. Spectra over the range 4000−450 cm^{-1} were obtained at a resolution of 1 cm^{-1} and a mirror velocity of 0.4583 cm s^{-1}. The FTIR analysis was performed to confirm the adsorption of alkylammonium ions and to identify the extent of hydrophobicity.

RESULTS AND DISCUSSION

Adsorption studies

The ability of the clay mineral to uptake a QAS was determined for different chain lengths. The adsorption density was plotted as a function of equilibrium QAS concentration (Figure 2). The adsorption isotherms were characterized by the three regions of interest: (1) the first region with a small slope indicating the adsorption of individual ions through ion exchange and electrostatic forces; (2) the rising part of the isotherm represents some ion exchange, but mostly dominated by hydrophobic chain-chain interactions; and (3) the onset of a plateau corresponding to the bilayer coverage.

The adsorption of HTAB rose very sharply, as clearly indicated by the second region of the curve (Figure 2).

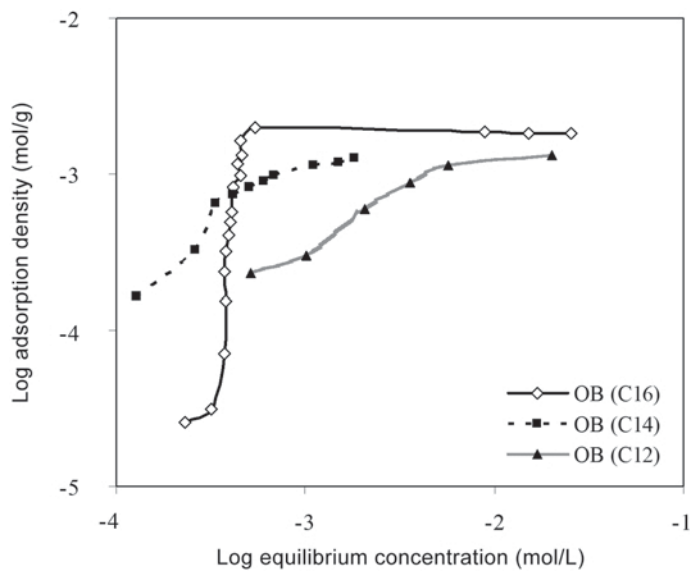

Figure 2. Adsorption density profiles of OB suspensions *vs.* log of equilibrium concentrations of amines.

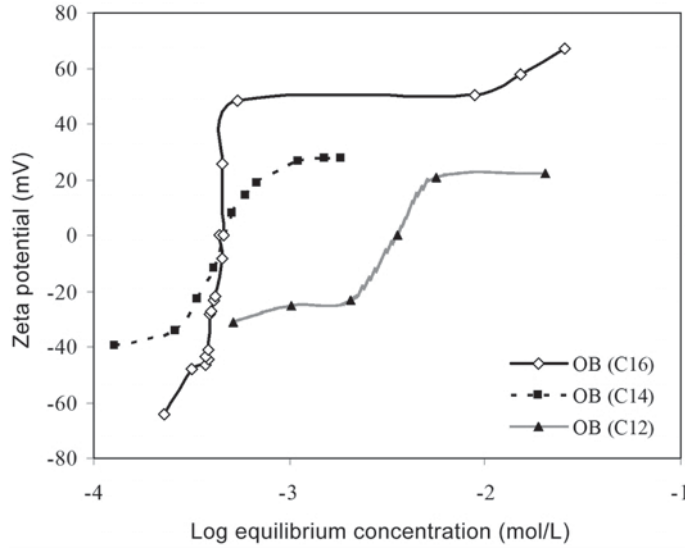

Figure 3. Zeta potential profiles of OB suspensions *vs.* log of equilibrium concentrations of amines.

Comparison of the adsorption plateaus observed for HTAB, TTAB, and DTAB revealed that the adsorption depended heavily on the chain length of the QAS, *i.e*. the greater the chain length, the greater the adsorption (Ersoy and Çelik, 2003; Yang *et al.*, 2002; Yılmaz and Yapar, 2004). However, in the rising parts of the isotherms the adsorption did not follow the same trend. In these areas, the adsorption of DTAB on the clay mineral was greater than that of TTAB, which was unexpected based on previous experience (Ersoy and Çelik, 2003; Yılmaz and Yapar, 2004). The characteristic changes in the clay surface, from hydrophilic to hydrophobic, are also difficult to explain according to the adsorption behaviors of DTAB and TTAB.

Characterization of OB suspensions

In order to confirm the extent of adsorption as a function of chain length, the zeta potential of the OB was measured. The zeta potentials showed nearly the same trend as the adsorption densities and verified the ability of QAS to adsorb on montmorillonite (Figure 3). The zeta potential of HTAB-modified OB was quickly reversed at the point where the adsorption density was high at the plateau (Figure 4). The last three points on the zeta potential curve of HTAB may refer to bilayer adsorption, which did not correlate well with the plateau part of the adsorption isotherm. However, the formation of bilayer has been reported in some studies (Ersoy and Çelik, 2003).

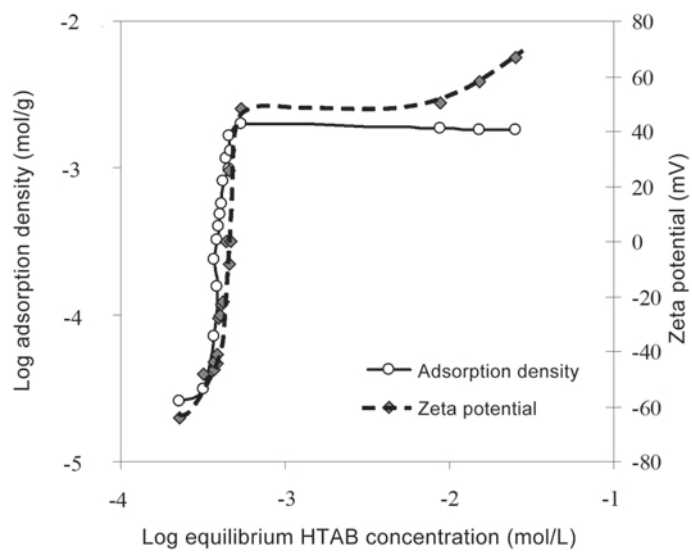

Figure 4. Adsorption density and zeta potential profiles of HTAB-modified OB *vs.* equilibrium concentration of amines.

The zeta potential profile of OB modified with DTAB (İşçi *et al.*, 2006) and TTAB exhibited charge reversal at the same concentration as did HTAB. The TTAB-modified OB experienced a charge reversal in the plateau region of the adsorption. In addition, the isoelectric point (IEP) initially decreased with increasing chain length (Somasundaran *et al.*, 1964) but then remained nearly constant (Figure 3). Decreases in the IEP also decreased the coagulation point, which prevented coagulation of the montmorillonite particles. Because of this, the surfactant can intercalate the clay mineral layers more efficiently.

The viscosity of HTAB-modified OB suspensions in water was very variable in the rising part of the adsorption isotherm (Figure 5) where the surface properties of the clay changed from hydrophilic to hydrophobic, *i.e.* the high viscosity represented the hydrophilic surface and the low viscosity denoted the hydrophobic surface. The last part of the curve where the viscosity increased may indicate the beginning of bilayer QAS adsorption. The viscosity of DTAB- and TTAB-modified OB suspensions in water showed similar variations to that of HTAB in the rising part of the adsorption isotherms. However, the viscosity of HTAB-modified OB suspension (Figure 4) increased while the viscosity of DTAB and TTAB-modified OB suspensions exhibited down peaks in the rising part of the adsorption isotherms. The down peaks observed for the viscosity of DTAB and TTAB-modified OB suspensions (Figure 5) indicated the hydrophobic state. The last parts of the curves after the down peaks showed the change in the clay mineral surface from hydrophobic to hydrophilic state.

Characterization of OB

The swelling behavior and hydrophobic character of OB were determined through swelling tests. The OB swelled well in toluene (Figure 6a) and swelling increased with increase in the initial concentration, in agreement with the expected increase in hydrophobicity. However, the DTAB-modified OB showed poor swelling and their suspensions did not exhibit any appreciable viscosity in water. This is in line with the hydrophobic nature of the DTAB-modified OB particles. The greatest swelling occurred at a 0.03 mol/L initial HTAB concentration. The level of swelling reached a maximum and then declined with increasing HTAB concentration. No appreciable change in the hydrophobicity of the clay at greater adsorption levels was evident. The variation in polarity was tested using a medium polarity fluid, acetone-toluene (50% v/v) (Figure 6b), the viscosity of which was between that of water and toluene.

The XRD analysis was used to determine the variation of basal spacing of OB as a function of QAS chain length and the CEC. The XRD profiles for the raw and the purified bentonite (unmodified) (Figure 7) revealed that the main smectite peak appears at 7º2θ for both samples and that impurities were removed upon purification.

The basal spacings of OB, modified at a 1:1 ratio of QAS to CEC, increased with increasing chain length (Figure 8a). HTAB-modified OB showed the largest basal spacing compared with other OB and unmodified bentonite. The variation in the basal spacing of different OB samples at QAS:CEC = 1 concentration (Figure 8a) were compared. The maximum basal spacing obtained at

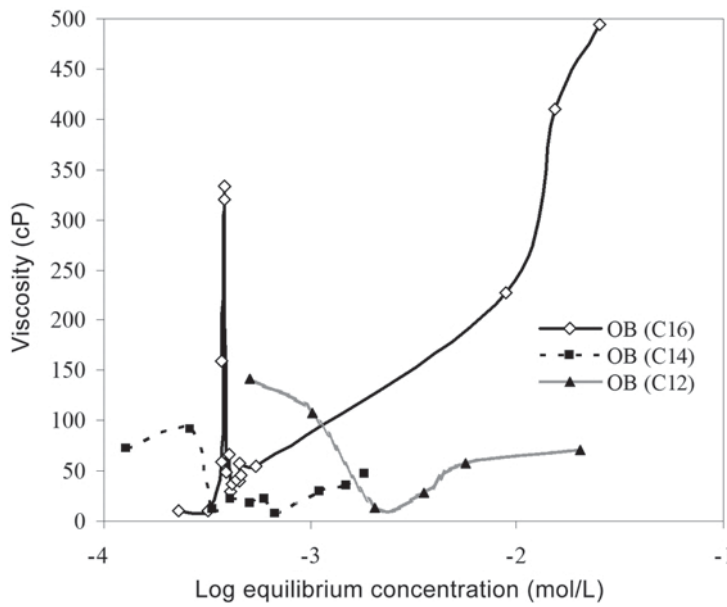

Figure 5. Viscosity variation of OB suspensions in aqueous solution *vs.* final concentrations of amines.

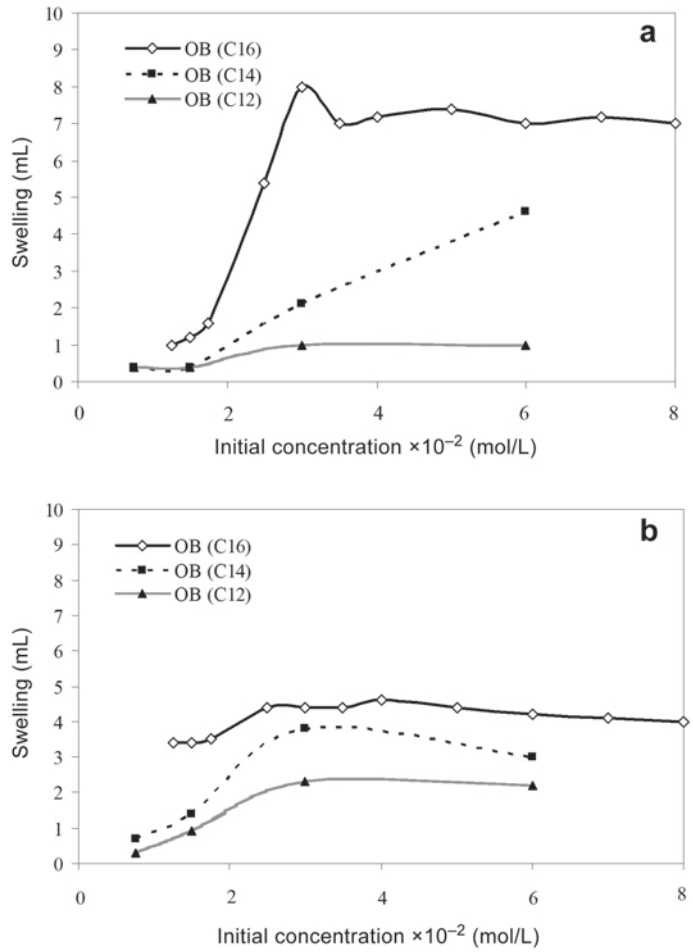

Figure 6. Swelling behavior of OB suspensions *vs.* the initial amine concentration: (a) in toluene, (b) in toluene + acetone (50% v/v).

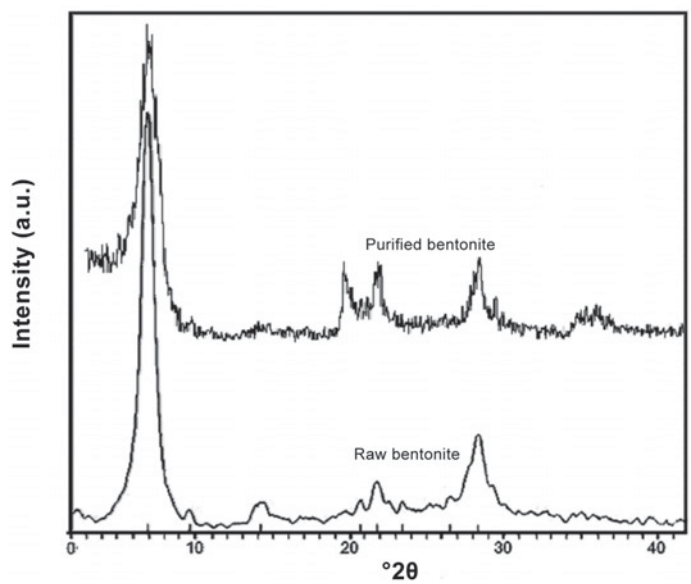

Figure 7. XRD patterns of raw and purified bentonite.

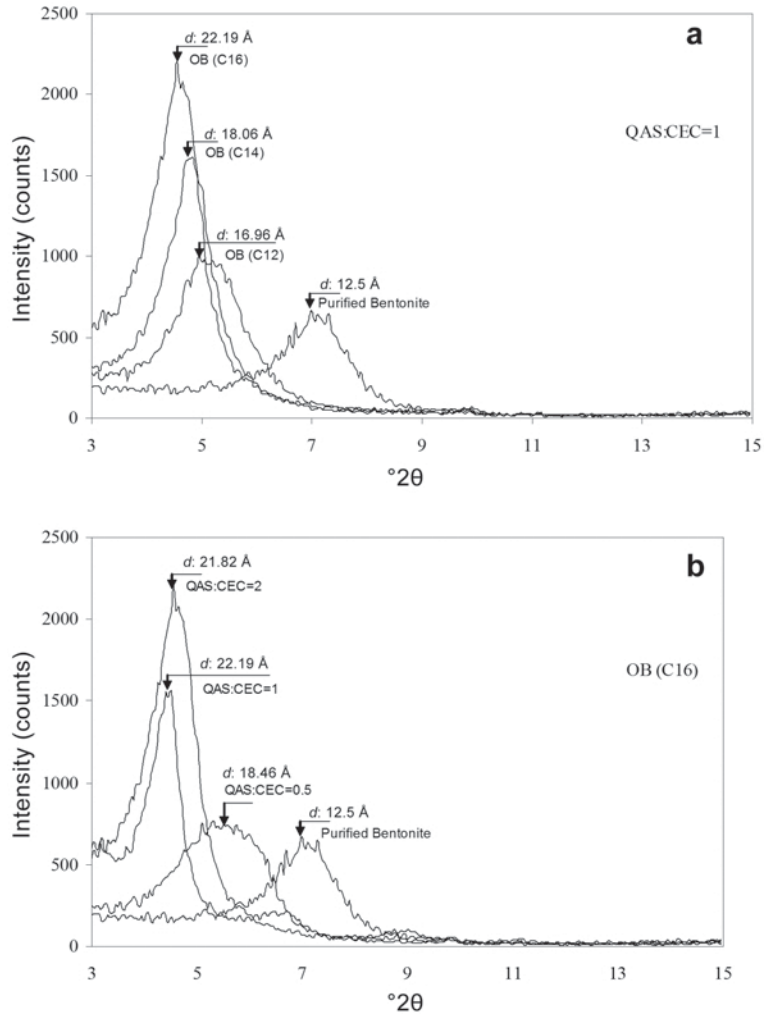

Figure 8. XRD patterns from purified bentonite compared with OB with different chain lengths (DTAB, TTAB, and HTAB): (a) QAS:CEC = 1, (b) at different HTAB:CEC ratios.

a QAS:CEC ratio of 1:1 represents the monolayer coverage. HTAB-modified OB showed the greatest basal spacing value of 22.19 Å compared with the unmodified bentonite (12.5 Å), the DTAB-modified (16.96 Å), and TTAB-modified (18.06 Å) OB (Figure 8a). The comparison between QAS showed that HTAB was more efficient for obtaining more expanded clay interlayers. Other than this, HTAB OB values were also compared in terms of the QAS:CEC ratios to determine the changes in basal spacing depending on QAS:CEC value in HTAB OB. The basal spacing increased linearly when QAS:CEC = 1; however, when QAS:CEC > 1 the basal spacing decreased (Figure 8b). The changes in basal spacings of OB depending on different QAS:CEC ratios and product type (Figure 9) also revealed that the basal spacing of OB increased with increasing QAS:CEC ratios and QAS chain length.

The SEM images (Figure 10) show the differences in structure between modified and unmodified bentonites.

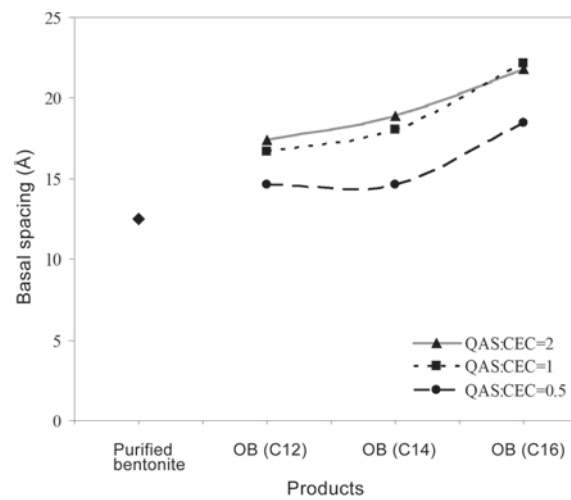

Figure 9. Change in basal spacing of unmodified and modified products at different QAS:CEC ratios.

The purified clay (Figure 10a) particles were single and sharp when compared with the modified clay particles (Figure 10b), which had a less defined structure, due perhaps to the QAS between the layers of the clay mineral.

The FTIR spectra of the purified bentonite in the absence and presence of QAS (Figure 11) were used to identify the nature of the interaction between bentonite and QAS. The FTIR spectra of the purified bentonite displayed a band at 3624 cm^{-1} due to structural O–H stretching vibrations; the band was independent of the cation type in the clay mineral interlayer suggesting that the exchange of interlayer cations had little effect on the structural OH in the octahedral sheet. The bands at 3433 cm^{-1} and 1637 cm^{-1} correspond to stretching and bending vibrations, respectively, of adsorbed water. The band at 1043 cm^{-1} derives from Si–O stretching vibrations. The peak at 917 cm^{-1} is greater by ~7 cm^{-1} than the band assigned to the Al–O–H bending mode, suggesting that Mg may have substituted for some of the Al in the octahedral sheet. The bands at 520 cm^{-1} and 470 cm^{-1} are assigned to Si–O–Al (octahedral Al) and Si–O–Si bending vibrations, respectively. The new or shifted bands in the OB were clearly visible after scale expansion (Figure 12a,b).

The QAS-OB showed peaks for H–O–H stretching and bending vibrations of adsorbed water at 3400–3430 cm^{-1} and 1637 cm^{-1}, originating from the clay structure and, to a lesser extent, from the QAS structure (Figure 12a). Bands from QAS were observed as follows: asymmetric and symmetric C–H stretching bands in the 2920–2955 cm^{-1} region (Figure 12b), CH_3-N asymmetric bending at 1487 cm^{-1} (Figure 12a), and

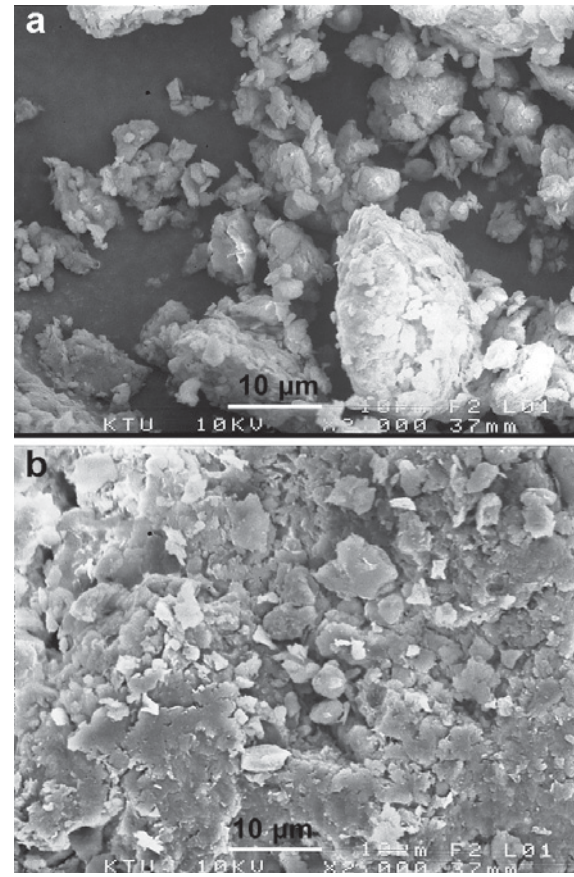

Figure 10. SEM images of (a) purified bentonite and (b) HTAB-modified OB at HTAB:CEC = 1.

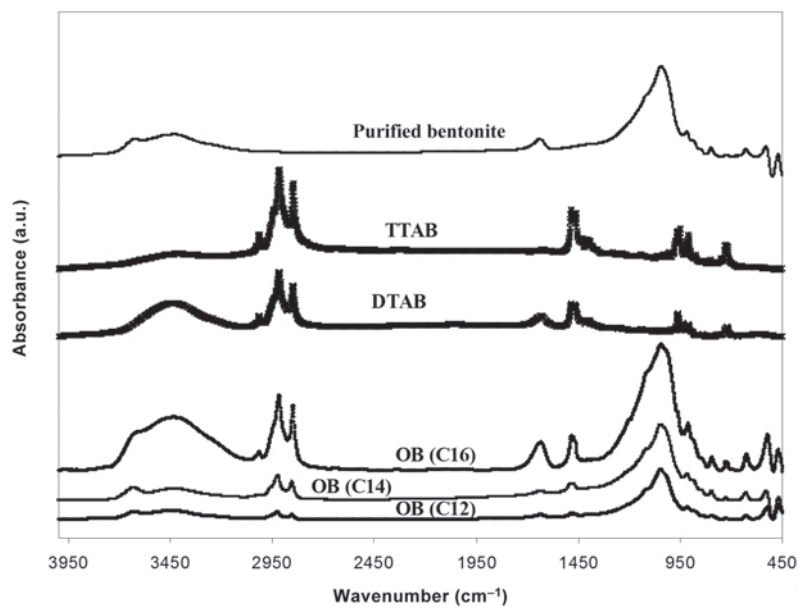

Figure 11. FTIR spectra of purified bentonite, TTAB, DTAB, and OB at QAS:CEC = 1.

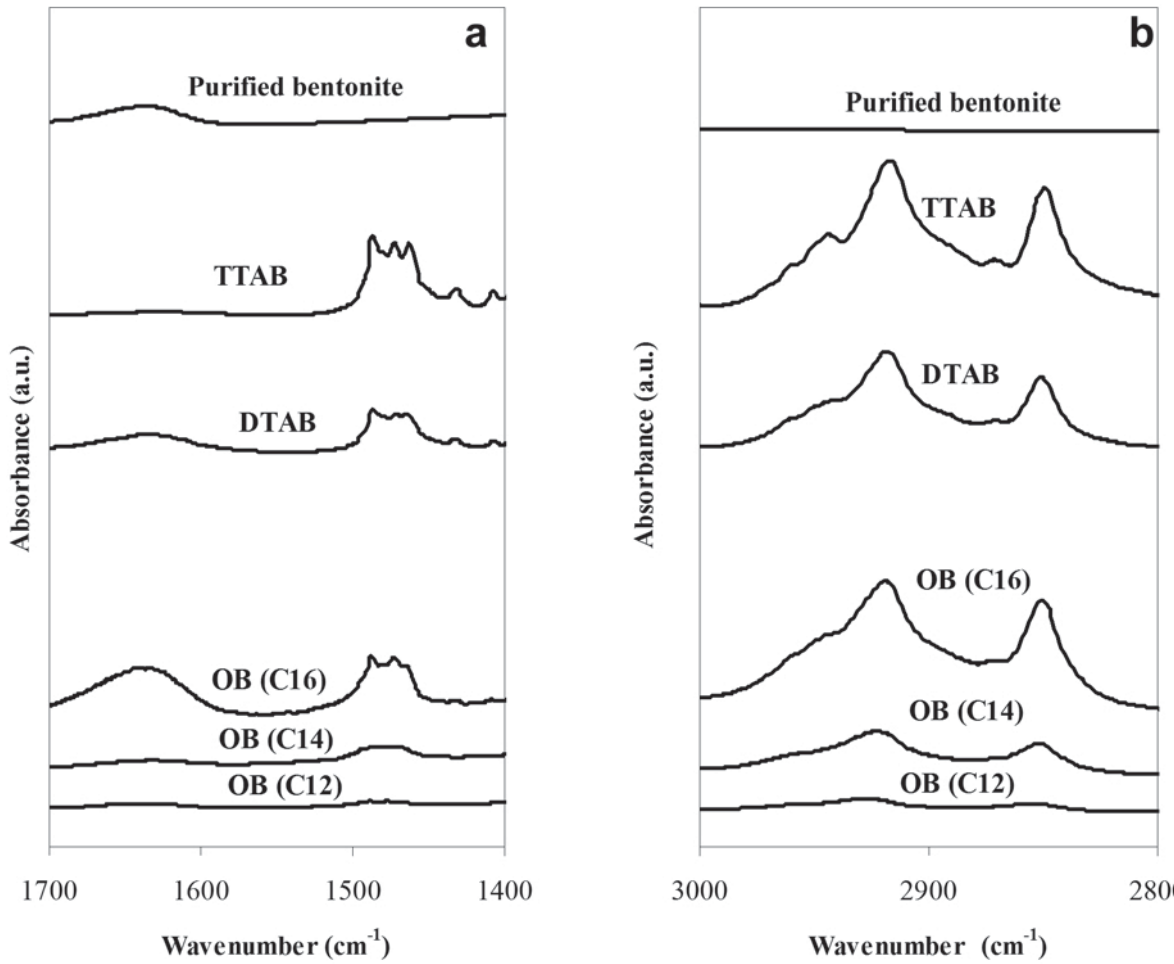

Figure 12. The newly formed peaks after the interaction between QAS and bentonite: (a) at 1487 cm^{-1} assigned to the CH_3-N asymmetric bending and adsorbed H-O-H vibrations at 1637 cm^{-1}; (b) C−H stretching bands at 2920−2955 cm^{-1}.

($(CH_2)_n$) in the 720 cm^{-1} region. Other peaks (3624 cm^{-1}, 3433 cm^{-1}, 1637 cm^{-1}, 1043 cm^{-1}, 917 cm^{-1}, 520 cm^{-1}, and 470 cm^{-1}) of the purified clay mineral do not appear due to overlap with the organic modes.

The patterns seen in the FTIR spectra marked as OB (C12), OB (C14), and OB (C16) (Figure 11) are attributed to the organically modified bentonites. The newly formed peaks (characteristic peak for $(CH_2)_n$ at 720 cm^{-1} (Figure 11), CH_3−N asymmetric bending at 1487 cm^{-1}, H–O–H vibrations at 3400−3430 cm^{-1} and at 1637 cm^{-1} (Figure 12a), and C−H stretching bands at 2920−2955 cm^{-1} (Figure 12b)) easily confirm the interaction between bentonite and the QAS.

CONCLUSIONS

The results from this study have indicated that the rate of adsorption of HTAB onto bentonite was greater than that of TTAB and DTAB. The zeta potential was increased as QAS adsorption increased and reached a plateau. Meanwhile the sign of the zeta potential was reversed from negative to positive. Although adsorption reached a plateau, the zeta potential continued to increase, which may be due to the onset of bilayer coverage. However, no such correlation was observed for the other QAS, probably because the energies are less favorable for the shorter-chain amines to form bilayers (Ersoy and Çelik, 2003; Yang *et al.*, 2002).

The viscosity of the OB suspensions showed a maximum in the region where the QAS adsorption increased sharply. The rising part of the isotherm also verifies the change in the zeta potential to a positively charged surface due to adsorption of excess alkylammonium ions. The trend of increase observed in the last part of the viscosity curve may indicate incipient bilayer alkylammonium adsorption. However, the viscosity of TTAB- and DTAB-modified OB increased after charge reversal to positive. Swelling tests revealed that the smaller the polarity, the greater the swelling of OB. The

greater swelling in toluene was attained for the HTAB-modified OB with monolayer coverage.

The basal spacing at the greatest expansion corresponded to the monolayer coverage, beyond which it remained roughly constant. The basal spacing of OB increased substantially with the addition of QAS and increasing the chain length of QAS; from 12.5 Å for the raw bentonite to 16.96 Å for DTAB- and 22.19 Å for HTAB-OB. These findings highlight the effect of the chain length of QAS on surface properties of OB.

ACKNOWLEDGMENTS

This research was supported by the Scientific and Technological Research Council of Turkey (TUBİTAK) 106G106 project. The authors thank Dr Feridun Boylu for his help with purification of the clay.

REFERENCES

Akın, Y. and Çelik, M.S. (1995) Electrokinetic behavior of montmorillonite type clays. Pp. 135–142 in: *Proceedings of the Industrial Raw Materials Symposium 95* (H. Köse and M.S. Kızıl, editors). The Chamber of Mining Engineers of Turkey, İzmir, Turkey (in Turkish).

Baldassari, S., Komarneni, S., Mariani, E., and Villa, C. (2006) Microwave versus conventional preparation of organoclays from natural and synthetic clays. *Applied Clay Science*, **31**, 134–141.

Boylu, F., Çinku, K., Çetinel, T., Erkan, İ., and Demirer, N. (2007) The separation efficiency of Reşadiye Na^+ bentonite by hydrocyclone. Pp. 213–227 in: *Proceedings of the 13th National Clay Symposium* (M. Kuşçu, O. Cengiz, and E. Şener, editors). Turkish National Committee on Clay Science, Van, Turkey (in Turkish).

Can, F., Erkan, İ., Yıldız, E., and Çelik, M.S. (2007) Organoclay preparation and characterization from Na^+ bentonites modified with cetyl pyridinium chloride (CPC) monohydrate. Pp. 365–377 in: *Proceedings of the 13th National Clay Symposium* (M. Kuşçu, O. Cengiz, and E. Şener, editors). Turkish National Committee on Clay Science, Van, Turkey (in Turkish).

Erkan, İ. (2008) Amine modification of Reşadiye bentonite and preparation of epoxy based nanocomposite (in Turkish). MSc thesis, Karadeniz Technical University, Trabzon, Turkey, 125 pp.

Erkan, İ., Alp, İ., Can, F.C., Karakaş, F., Çelik, M.S., and Yüzer, H. (2008) Adsorption, rheology and electrokinetic properties of organo modified sodium bentonites from Reşadiye region. Pp. 743–748 in: *Proceedings of the 11th International Mineral Processing Symposium* (G. Özbayoğlu, A.İ. Arol, Ç. Hoşten, and Ü. Atalay, editors). Turkish Mining Development Foundation, Antalya, Turkey.

Ersoy, B. and Çelik, M.S. (2003) Effect of hydrocarbon chain length on adsorption of cationic surfactants onto clinoptilolite. *Clays and Clay Minerals*, **51**, 173–181.

Faci, H. (2001) Open gear lubricants. *US Patent 6251839*.

Favre, H. and Lagaly, G. (1991) Organo-bentonites with quaternary alkylammonium ions. *Clay Minerals*, **26**, 19–32.

Forland, G.M. and Blokhus, A.M. (2007) Adsorption of phenol and benzyl alcohol onto surfactant modied silica. *Journal of Colloid and Interface Science*, **310**, 431–435.

Frost, R., Xi, Y., and He, H. (2007) Modification of the surfaces of Wyoming montmorillonite by the cationic surfactants alkyl trimethyl, dialkyl dimethyl and trialkyl methyl ammonium bromides. *Journal of Colloid and Interface Science*, **305**, 150–158.

Gorassi, G., Tortora, M., Vittoria, V., Kaempfer, D., and Mülhaupt, R. (2003) Transport properties of organic vapor in nanocomposites of organophilic layered silicate and syndiotactic polypropylene. *Polymer*, **44**, 3679–3685.

İşçı, S., Ece, Ö.I., and Güngör, N. (2006) Characterization of rheology, electrokinetic properties, and surface micromorphology of DTABr-MMT and CPBr-MMT organoclays. *Journal of Composite Materials*, **40**, 1105–1115.

Kirsner, J., Miller, J., and Bracken, J. (2003) Additive for oil-based drilling fluids. *US Patent 6620770*.

Klapyta, Z., Fujita, T., and Iyi, N. (2001) Adsorption of dodecyl- and octadecyltrimethylammonium ions on a smectite and synthetic micas. *Applied Clay Science*, **19**, 5–10.

Klapyta, Z., Gawel, A., Fujita, T., and Iyi, N. (2003) Structural heterogeneity of alkylammonium-exchanged, synthetic fluorotetrasilicic mica. *Clay Minerals*, **38**, 151–160.

Lagaly, G. (1986) Interaction of alkylamines with different types of layered compounds. *Solid State Ionics*, **22**, 43–51.

Lagaly, G., Ogawa, M., and Dekany, I. (2006) Clay Mineral Organic Interactions. Pp. 309–377 in: *Handbook of Clay Science, Developments in Clay Science, Vol.1* (F. Bergaya, B.K.G. Theng, and G. Lagaly, editors). Elsevier, Amsterdam.

Lan, T. and Pinnavaia, T.J. (1994) Clay-reinforced epoxy nanocomposites. *Chemistry of Materials*, **6**, 2216–2219.

Lee, J.F., Crum, J.R., and Boyd, S.A. (1989) Enhanced retention of organic contaminants by soils exchanged with organic cations. *Environmental Science and Technology*, **23**, 1365–1372.

Liu, W., Hoa, S.V., and Pugh, M. (2005) Organoclay-modied high performance epoxy nanocomposites. *Composites Science and Technology*, **65**, 307–316.

Marras, S.I., Tsimpliaraki, A., Zuburtikudis, I., and Panayiotou, C. (2007) Thermal and colloidal behavior of amine-treated clays: The role of amphiphilic organic cation concentration. *Journal of Colloid and Interface Science*, **315**, 520–527.

Medrzycka, K. and Zwierzykowski, W. (2000) Adsorption of alkyltrimethylammonium bromides at the various interfaces. *Journal of Colloid and Interface Science*, **230**, 67–72.

Mohammad, A. and Bhawani S.A. (2008) LC separation of co-existing cetylpyridinium chloride, tetradecyltrimethylammonium bromide and dodecyltrimethylammonium bromide on silica TLC plates with aqueous-organic eluents. *Chromatographia*, **67**, 659–663.

Nuntiya, A., Sompech, S., Aukkaravittayapun, S., and Pumchusak, J. (2008) The effect of surfactant concentration on the interlayer structure of organoclay. *Chiang Mai Journal of Science*, **35**, 199–205.

Paiva, L.B., Morales, A.R., and Diaz, F.R.V. (2008) Organoclays: properties, preparation and applications. *Applied Clay Science*, **42**, 8–24.

Patel, H.A., Somani, R.S., Bajaj, H.C., and Jasra, R.V. (2006) Nanoclays for polymer nanocomposites, paints, inks, greases and cosmetics formulations, drug delivery vehicle and waste water treatment. *Bulletin of Materials Science*, **29**, **2**, 133–145.

Reid, V.W., Longman, G.F., and Heinerth, E. (1967) Determination of anionic active detergents by two phase titration. *Tenside Surfactants Detergents*, **4**, 292–304.

Sabah, E., Kara, M., Hancer, M., and Çelik, M.S. (1998) Adsorption mechanism of organic and inorganic ions by a clay absorbent: sepiolite, Preprint No. 98–152 in: *SME Annual Meeting*, Florida.

Sabah, E., Mart, U., Çınar, M., and Çelik, M.S. (2007) Zeta potentials of sepiolite suspensions in concentrated monovalent electrolytes. *Separation Science and Technology*, **42**, 2275–2288.

Smith, J.A., Jaffe, P.R., and Chlou, C.T. (1990) Effect of ten quaternary ammonium cations on tetrachloromethane sorption to clay from water. *Environmental Science and Technology*, **24**, 1167–1172.

Somasundaran, P., Healy, T.W., and Fuerstenau, D.W. (1964) Surfactant adsorption at the solid-liquid interface-dependence of mechanism on chain length. *The Journal of Physical Chemistry*, **68**, 3562–3566.

Sompech, S., Nuntiya, A., Aukkaravittayapun, S., and Pumchusak, J. (2008) Interlayer expansion of organoclay by cationic surfactant. *Chiang Mai University Journal of Natural Science Special Issue on Nanotechnology*, **7**, 89–93.

Tjandra, W., Yao, J., and Tam, K.C. (2006) Interaction between silicates and ionic surfactants in dilute solution. *Langmuir*, **22**, 1493–1499.

Vazquez, A., Lopez, M., Kortaberria, G., Martin, L., and Mondragon, I. (2008) Modification of montmorillonite with cationic surfactants. Thermal and chemical analysis including CEC determination. *Applied Clay Science*, **41**, 24–36.

Vougaris, D. and Petridis, D. (2002) Emulsifying effect of dimethyldioctadecylammonium-hectorite in polystyrene/poly(ethyl methacrylate) blends. *Polymer*, **43**, 2213–2218.

Xi, Y., Martens, X., He, H., and Frost, R.L. (2005) Thermogravimetric analysis of organoclays intercalated with the surfactant octadecyltrimethylammonium bromide. *Journal of Thermal Analysis and Calorimetry*, **81**, 91–97.

Xie, W., Gao, Z., Liu, K., Pan, W.-P., Vaia, R., Hunter, D., and Singh, A. (2001) Thermal characterization of organically modified montmorillonite. *Thermochimica Acta*, **367–368**, 339–350.

Yang, L., Jiang, L., Zhou, Z., Chen, Y., and Wang, X. (2002) The sedimentation capabilities of hexadecyltrimethylammonium-modied montmorillonites. *Chemosphere*, **48**, 461–466.

Yılmaz, N. and Yapar, S. (2004) Adsorption properties of tetradecyl- and hexadecyl trimethylammonium bentonites. *Applied Clay Science*, **27**, 223–228.

Zhu, L., Li, Y., and Zhang, J. (1997) Sorption of organobentonites to some organic pollutants in water. *Environmental Science and Technology*, **31**, 1407–1410.

Zhu, L., Zhu, R., Xu, L., and Ruan, X. (2007) Influence of clay charge densities and surfactant loading amount on the microstructure of CTMA-montmorillonite hybrids. *Colloids and Surfaces A: Physicochemical and Engineering Aspects*, **304**, 41–48.

(*Received 25 May 2010; revised 8 November 2010; Ms. 439; A.E. F. Bergaya*)